京都大学防災研究所年報 第 49 号 B 平成 18 年 4 月
Annuals of Disas. Prev. Res. Inst., Kyoto Univ., No. 49 B, 2006

Effect of Large Tidal Variation on Storm Surge

Soo Youl KIM*, Tomotsuka TAKAYAMA and Tomohiro YASUDA

* Graduate School of Urban and Environment Engineering, Kyoto University

Synopsis

This study investigates the effect of large tidal variation on storm surge in the coastal sea of western Korea which has a complex bathymetry and a large tidal variation. Storm surge should randomly occur at high, low and intermediate tides. The large tidal variation affects the magnitude of storm surge in a very shallow and wide coast sea. Therefore the coupled model is developed to allow the data exchange among surge/tide models and wave model (SWAN). The investigations are made on the relation of the storm surge and the tide and the effect of large tidal variation on radiation stress. The coupled model was applied to hindcast storm surge by Typhoon Rammasun (T0205) which hit the west of Korea in 2002. The results of the coupled model conclude that the relation of both them is non linear and they are strongly coupled each other.

Keywords: Storm surge, tide, radiation stress, coupling model, SWAN

1. Introduction

The Korean Peninsula located between the East Sea (Japan Sea) and the Yellow Sea has the coastline of 17,300km and the offshore islands of 3,418. The west coast is an area of geological submergence which has produced many head lands, bays and hundreds of islands. Tidal flats up to 1,700km^2 in the west coast are exposed at low tide and a large tidal variation reaches up to 10m in the Kyunggi Bay. Typhoons which hit the Korean Peninsula also pass through the west or south to the east or north of it from July to August as shown in Fig.1. Therefore storm surge superimposed on high tide gives more severe condition to a coastal region. Consequently the inundation and damage due to typhoon have especially occurred in the south and west coast.

Since Janssen (1989, 1991) introduced quasi-linear theory of wind-wave generation, significant efforts were made on the surge simulation in terms of various interaction mechanisms among wave, surge and tide in their coupling model. Mastenbroek et al. (1993) clearly show the influence of a wave-dependent surface drag coefficient on surge elevations. Ozer et al. (2000) applied their own developed generic module to the North Sea and the Spanish coast and showed that the sensitivity of waves increases due to the coupling with tide and surge in shallow sea more than in deep sea. M. Y. Zhang and Li (1995) investigated the mutual interaction of waves and currents in the South and East China Seas. Choi (2003) first attempted the effect of tides, storm surges and wind waves interaction in the Yellow Sea that the effective drag coefficient of the bottom stress is determined from an iterative process followed by the method of Grant and Madsen (1986). However, this method tends to overestimate the current bottom stress in comparison with the wave bottom stress (Kagan et al., 2005)

In this study, how a large tidal variation influences on storm surge is investigated by considering the interaction of the wave, surge and tide. In order to compute the wave transformation, storm surge and tide, the coupling model of SWAN (Simulating WAves Nearshore) and a

non-linear long wave equation for storm surge was developed. The model was applied to the hindcasting simulation of storm surge generated by Typhoon Rammasun (T0205) which hit the western coastal region in 2002.

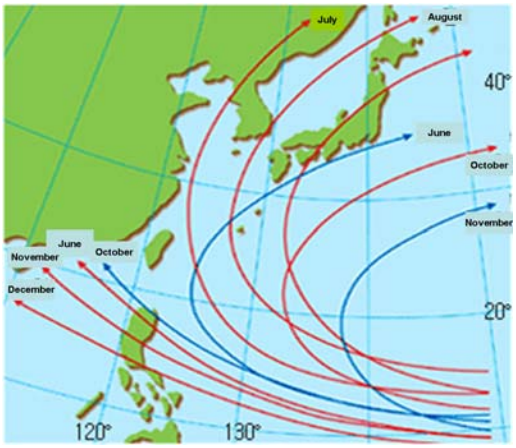

Figure 1. Typhoon tracks around the Korean Peninsula (from Korean Meteorological Administration)

2. Numerical model

2.1 Wave model

A third-generation numerical wave model (SWAN) to compute random, short-crested waves in coastal regions with shallow water and ambient current was developed and verified by N. Booij et al. (1999). The model can be applied to coastal regions with shallow water, islands, tidal flats and local wind as well as with horizontal scales less than 20-30km and water depth less than 20-30m. This model accounts for shoaling, refraction, generation by wind, whitecapping, triad and quadruplet wave-wave interactions, and bottom and depth-induced wave breaking. The basic equation in SWAN is the wave action balance equation and is given by

$$\frac{\partial}{\partial t}N+\frac{\partial}{\partial x}c_x N+\frac{\partial}{\partial y}c_y N+\frac{\partial}{\partial \sigma}c_\sigma N+\frac{\partial}{\partial \theta}c_\theta N=\frac{S}{\sigma} \quad (1)$$

in the Cartesian coordinates (x, y). Here, $N(\sigma, \theta)$ is the action density spectrum, c_x and c_y present the propagation velocities in x and y direction, c_σ and c_θ also present the one in σ and θ direction and S is the source terms. t is the time, x and y present the space in geographic grid, in contrast with σ and θ are the frequency and its direction of a wave component.

The first term on the left side of Eq. (1) represents the local rate of change of action density in time, the second and third term represent propagation of action in x and y space, respectively. The fourth term represents shifting of the relative frequency due to variation in depths and currents. The fifth term represents wave refraction induced by sea depth and current. All terms except first one include the propagation velocity in geographical, σ and θ space. The term $S(\sigma, \theta)$ at the right-hand side of Eq. (1) is the source term in terms of energy density, representing the effects of generation, dissipation and nonlinear wave-wave interactions.

Time is discretized with a simple constant time step for the simultaneous integration of the propagation and the source terms in contrast with it in the WAM model or the WAVEWATCH model. The discrete frequencies are defined between a fixed low-frequency cutoff (typically, f_{min}=0.04Hz) and a fixed high-frequency cutoff (typically, f_{max}=1.0Hz) which are defined by the user or computed by SWAN, respectively. SWAN allows the use of nested grids to provide high-resolution results at desired locations and provides estimates of wave setup due to radiation stress.

2.2 Storm surge and tide model

The depth-integrated, non-linear long wave equations in the Cartesian coordinates is given by

$$\frac{\partial \eta}{\partial t}+\frac{\partial M}{\partial x}+\frac{\partial N}{\partial y}=0 \quad (2)$$

$$\frac{\partial M}{\partial t}+\frac{\partial}{\partial x}\left(\frac{M^2}{d}\right)+\frac{\partial}{\partial y}\left(\frac{MN}{d}\right)+gd\frac{\partial}{\partial x}(\eta-\eta_0)=$$
$$fN-\frac{1}{\rho}d\frac{\partial P}{\partial x}+\frac{1}{\rho}(\tau_s^x-\tau_b^x+F_x)+A_h\left(\frac{\partial^2 M}{\partial x^2}+\frac{\partial^2 M}{\partial y^2}\right) \quad (3)$$

$$\frac{\partial N}{\partial t}+\frac{\partial}{\partial x}\left(\frac{NM}{d}\right)+\frac{\partial}{\partial y}\left(\frac{N^2}{d}\right)+gd\frac{\partial}{\partial y}(\eta-\eta_0)=$$
$$-fM-\frac{1}{\rho}d\frac{\partial P}{\partial y}+\frac{1}{\rho}(\tau_s^y-\tau_b^y+F_y)+A_h\left(\frac{\partial^2 N}{\partial x^2}+\frac{\partial^2 N}{\partial y^2}\right) \quad (4)$$

where η = the sea surface elevation, M and N = the depth integrated currents in the x and y direction, P = the atmospheric pressure, f = the Coriolis parameter, g = the gravitational acceleration, $d=\eta+h$ = the total depth, A_h = the horizontal eddy diffusion and ρ = the density of water. F_x and F_y represent the components of the wave

induced force which are the function of the radiation stress in x and y space. At next section 2.4, those will be explained in details. The bottom stresses is given by

$$\tau_b = \rho_w g n^2 \frac{U|U|}{d^{7/3}} \tag{5}$$

where n is the Manning coefficient. The surface stress is usually given by

$$\tau_s = \rho_a C_D W_{10} |W_{10}| \tag{6}$$

where W_{10} is the measured wind speed at 10m. In coupling model, this equation will be replaced by a more elaborate form which will be also explained at next section 2.4.

Eqs. (2) and (3) are discretized in space on the staggered Arakawa C grid and in time using leap-frog method. The difference scheme is explicit and uses the first order central derivative for space and forward derivative for time. The nonlinear advective terms and the horizontal friction terms are computed by the first order upwind - central derivative and the second order one, respectively.

The boundary condition is zero flow normal to a solid boundary and a radiation condition is applied to open boundary and the disturbed water surface at an open boundary is given by

$$\eta_n = \eta_{tide} + \eta_{storm\ surge} \tag{7}$$

where $\eta_{storm\ surge}$ is assumed as follows:

$$\eta_{storm\ surge} = (p_a - p_0)/g\rho \tag{8}$$

where p_a and p_0 represent 1013mb and the atmospheric pressure at the open boundary. η_{tide} is imposed by ocean tide model for a regional model around Japan (Koji, 2000) which can make the realistic tide predict. The wet/dry scheme is also applied for the sake of tidal flat simulation.

2.3 Typhoon model (Fujita model)

The pressure field in the typhoon is determined by

$$p = p_\infty - \frac{\Delta p}{\sqrt{1 + (r/r_0)^2}} \tag{9}$$

where p_∞ and Δp represent 1013mb and the pressure differential, and r and r_0 denote the radial distance from the typhoon center and the radius of maximum wind speed, respectively. The speed of wind is calculated by

$$V_{gr} = r\left[\sqrt{\frac{f^2}{4} + \frac{\Delta p}{\rho_a r_0^2}\left\{1 + \left(\frac{r}{r_0}\right)^2\right\}^{-3/2}} - \frac{f}{2}\right] \tag{10}$$

where f is the Coriolis coefficient and the rest are same with those in Eq. (12). The radius of maximum wind speed, r_0 was estimated using the pressure data observed at 76 meteorological stations in Korea.

2.4 Surface wind stress and Radiation stress

The radiation stress tensor S_{ij} represents contribution of the wave motion to the mean flux of horizontal momentum, which will be explicitly expressed in terms of the wave spectrum E as

$$S_{xx} = \rho g \int\int \left[\frac{C_g}{C}\cos^2\theta + \frac{C_g}{C} - \frac{1}{2}\right] E d\sigma d\theta \tag{11}$$

$$S_{xy} = S_{yx} = \rho g \int\int [\cos\theta \sin\theta] E d\sigma d\theta \tag{12}$$

$$S_{yx} = \rho g \int\int \left[\frac{C_g}{C}\cos^2\theta + \frac{C_g}{C} - \frac{1}{2}\right] E d\sigma d\theta . \tag{13}$$

The wave induced forces in Eqs. (3) and (4) are represented by

$$F_x = -\frac{\partial S_{xx}}{\partial x} - \frac{\partial S_{xy}}{\partial y} \tag{14}$$

$$F_y = -\frac{\partial S_{yx}}{\partial x} - \frac{\partial S_{yy}}{\partial y} \quad . \tag{15}$$

Janssen (1991) described the effect of wind generated gravity waves on the airflow and especially introduced that for young wind sea, a strong interaction between wind and wave is found, resulting in a substantial

increase of the stress in the surface layer. In general, the total stress is the sum of a turbulent and a wave-induced stress as follows

$$\tau = \tau_{turb} + \tau_w . \tag{16}$$

Here, τ_{turb} is the turbulent stress, which is modeled by a mixing length hypothesis,

$$\tau_{turb} = \rho_a (\kappa z)^2 \left(\frac{\partial U}{\partial z} \right)^2 \tag{17}$$

where κ (=0.4) is the von Karman constant and $U(z)$ the wind speed at height z. Based on the numerical results of Janssen (1989), the wind profile still has a logarithmic shape for the young wind sea. The wind profile is assumed as follows

$$U(z) = \frac{u_*}{\kappa} \ln \left(\frac{z + z_e - z_0}{z_e} \right) \tag{18}$$

and

$$u_* = \sqrt{\tau / \rho_a} . \tag{19}$$

where u_* is the friction velocity and z_0 represents the roughness length. The effective roughness length z_e at $z = z_0$ depends on z_0 and the sea state through the wave induced stress τ_w and the total surface stress τ.

$$z_e = \frac{z_0}{\sqrt{1 - \tau_w / \tau}} \tag{19}$$

and

$$z_0 = \hat{\alpha} \frac{u_*^2}{g} . \tag{20}$$

Eq. (20) is a Charnock-like relation. Since the drag coefficient, defined by

$$C_D = u_*^2 / U(L)^2 , \tag{21}$$

is fully determined by the roughness length where $U(L)$ is the wind speed given at L . Therefore the total surface stress τ is given by

$$\tau = C_D U(L)^2 \tag{22}$$

The wave stress τ_w vector is determined by

$$\tau_w = \rho_w \int_0^{2\pi} \int_0^{\infty} \omega S_{in}(\sigma, \theta) \frac{\bar{k}}{k} d\sigma d\theta \tag{23}$$

where ω is the angular frequency, S_{in} is the wind input source function, and k and $\bar{k}$ represent the wave-number and the mean wave-number of a wave component, respectively.

In the SWAN model the iterative procedure of Mastenbroek et al. (1993) is used. Through this iterative procedure from Eqs. (18) to (23) the surface stress is determined. As a Consequence, the ratio τ_w / τ depends on the wave age and denotes the interaction between the wind and the wave. Hence, the surface stress will be enhanced in the young wind sea than the old wind sea.

2.5 Coupling procedures

For the tide and storm surge simulation, the depth integrated equations was employed, while SWAN model was used for wave prediction. The coupling scheme of the two models is shown in Fig. 2

(1) The surge/tide model preliminary computes the tide in the domain.
(2) The wave model is run under the velocities and water surface elevation from (1) to obtain the waves.
(3) The surge/tide model is re-run by the modified wind stress and the calculated wave radiation stress from (2).
(4) New velocity and water surface elevation are given for the wave model.

The procedure (2)-(4) are repeated. The time step for the exchange of the data between surge/tide and wave is chosen 100 seconds. For the storm/tide model the time step of 5 seconds is employed, while 100 seconds is used on SWAN at the time step.

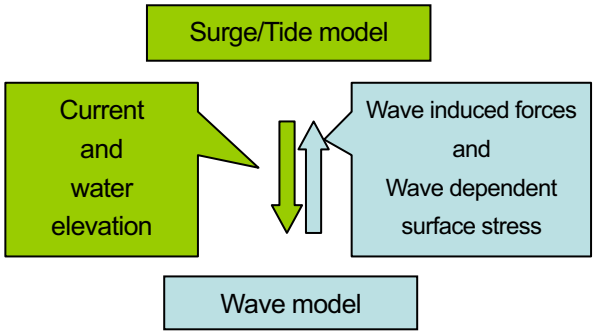

Figure 2. The schematic diagram of synchronous coupling model

3. Application to the west sea of Korea

3.1 Typhoon of Rammasun

The track of the typhoon Rammasun (T0205) which was born on UTC 28 June 2002 near 10° N 138° E is shown in Fig. 3. At 06:00 1 July 2002 the tropical storm changed to the typhoon and at 00:00 5 July 2002 it again returned to tropical storm. Typhoon Rammasun hit the west sea in the Korea on UTC 6 July 2002.

3.2 Modeled region

The case study provides effect of large tidal variation on storm surge in the west sea of Korea. Fig. 4 shows the computational domain and bathymetry from 117° E to 132° E and from 30° N to 41° N with a resolution of 7,800m. The computational domain covers a large ocean surface including the west coast of the study site to make it to take sufficient time and fetch for the generation of the wind wave through the numerical simulation. The model has 226×166 grid elements. The three points for investigation is shown in figure 4. Two points of A and C represent the tide observation point at Yonggwang and Boryeong where have been set up at the head land on Korean Peninsula, while B has been installed at Weido island. The tidal ranges are approximately up to 4m at three positions during the storm event.

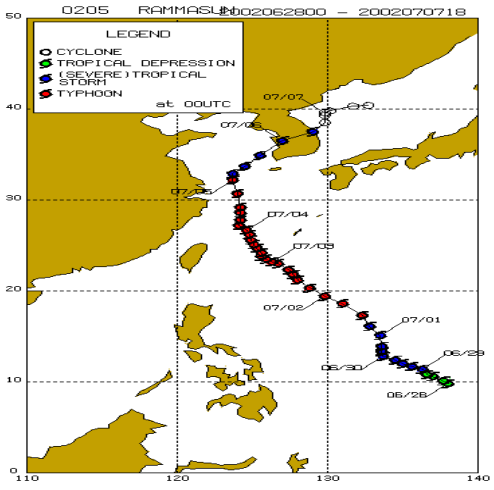

Figure 3. Path of Rammasun (T0205) in 2002

4. Discussion

The surge, wind wave and tide were hindcasted for the typhoon of Rammasun (T0205) for 5days starting from 00:00 UTC 3 July just before the center of Rammasun crossed into the computation domain at 30° N from the south. Before the coupling procedure starts, the tide is first calculated to set-up the steady state.

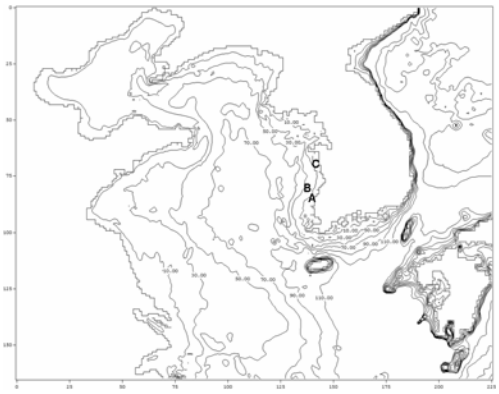

Figure 4. Modeled region with three observation positions

Once the tide is sufficiently steady, the coupling model begins to calculate the storm surge and wave propagation with tide imposition at open boundary.

Since only storm surge data are available, the computed total water elevations were compared with field data. Results at the points of A, B and C under two different forcing conditions in the storm surge model are shown in Fig. 6(b), 7(b) and 8(b) to investigate the effect of the radiation stress on storm surge; One is the model to consider the wave radiation stress and the modified wind stress and the other is the model to do only the wind stress.

Fig. 5 shows the significant wave heights from the results considering the modified wind stress and the radiation stress at the points of A, B and C. It can be seen from Fig. 6, 7 and 8 that the negative storm surges lower than the tidal level occur at the high tide, while the positive storm surges occur at the low tide. The negative storm surge is supposed to be caused by the very small atmospheric pressure depression of the typhoon. The effect of the radiation stress is also varied along with the storm surge and the observed point, and the order of it varies approximately 10% to 1% of coinciding with the positive storm surge. Therefore it is hard to say whether the effect of the radiation stress is significant or not yet, because the results are obtained from only one typhoon data.

However, it is significantly confirmed that tidal variation influenced strongly on the storm surge at the points of A, B and C.

5. Conclusions

The coupling model of a third generation wave model (SWAN) and a non linear long wave model is developed to investigate the effect of a large tidal variation on a storm surge at the west coast of Korea.

The computed results show that the large tide and the storm surge are strongly coupled. The radiation stress influences slightly on the storm surge. Therefore it is need to investigate the effect of radiation stress by the high resolution and more typhoon data because of a lot of islands and a complex geographic.

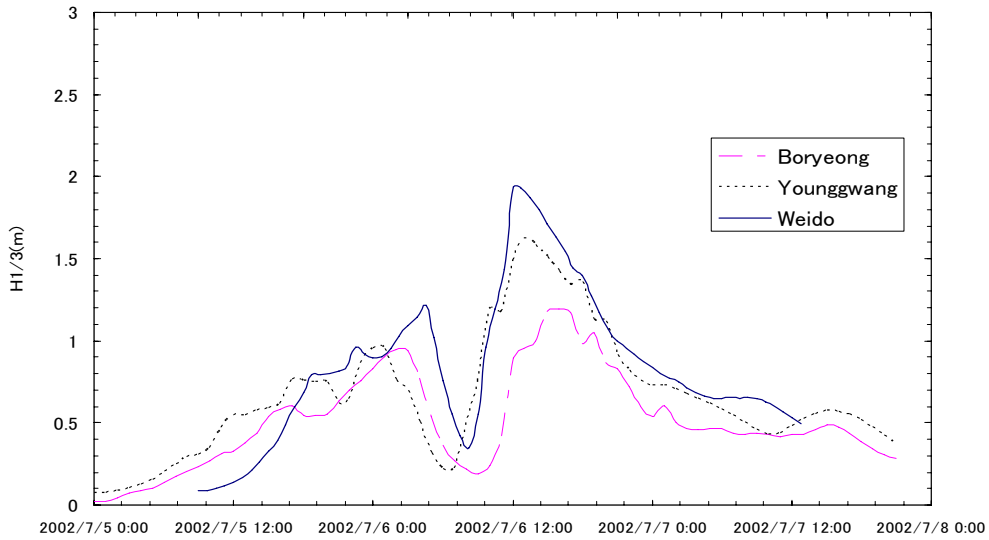

Figure 5. The significant wave heights

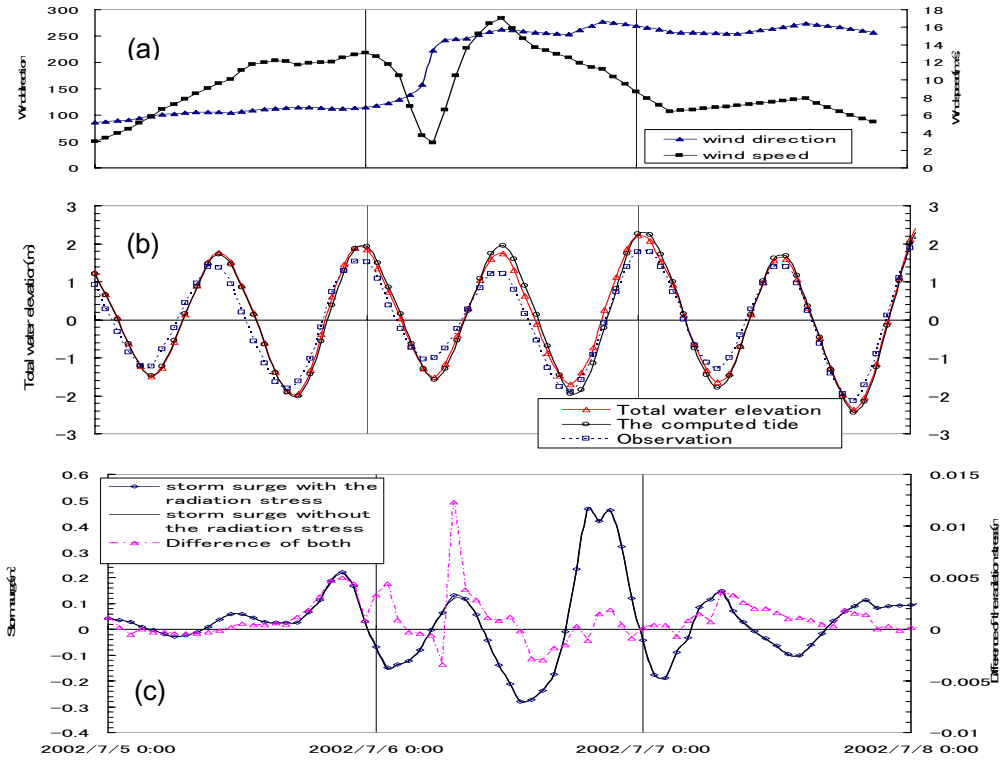

Figure 6. (a) the wind direction and speed; (b) the total water elevation of observation, the only computed tide and the computed total water elevation with the radiation stress; (c) the only storm surge considering the radiation stress, one without the radiation stress and difference of both at A (Yonggwang).

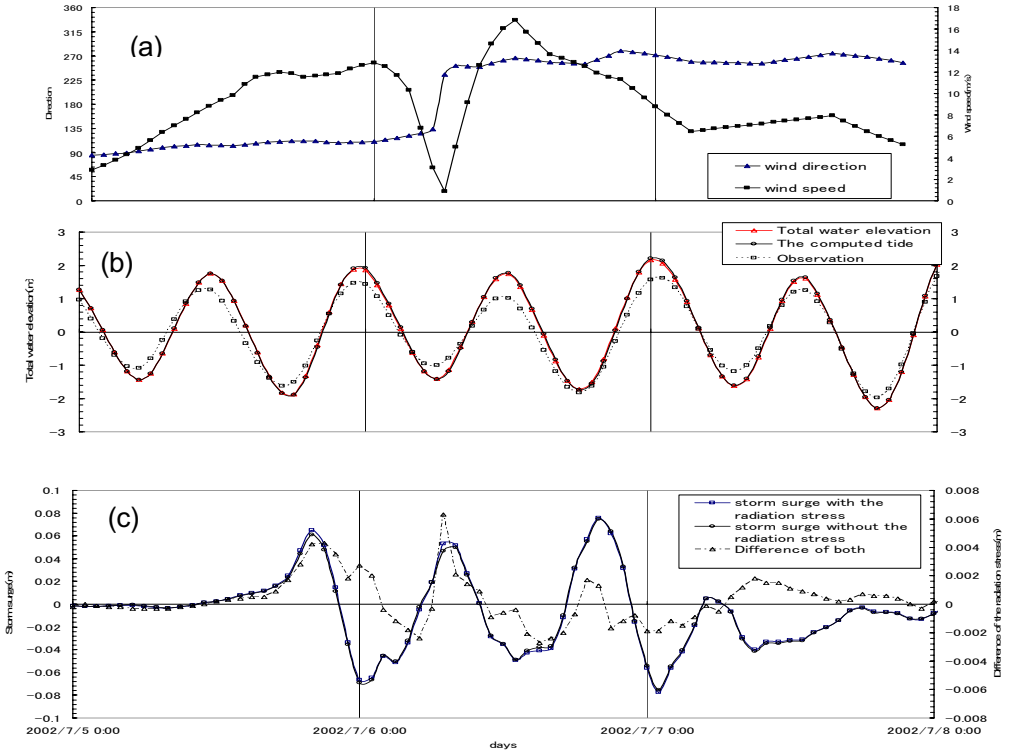

Figure 7. The same with Fig. 5 but at B (Weido)

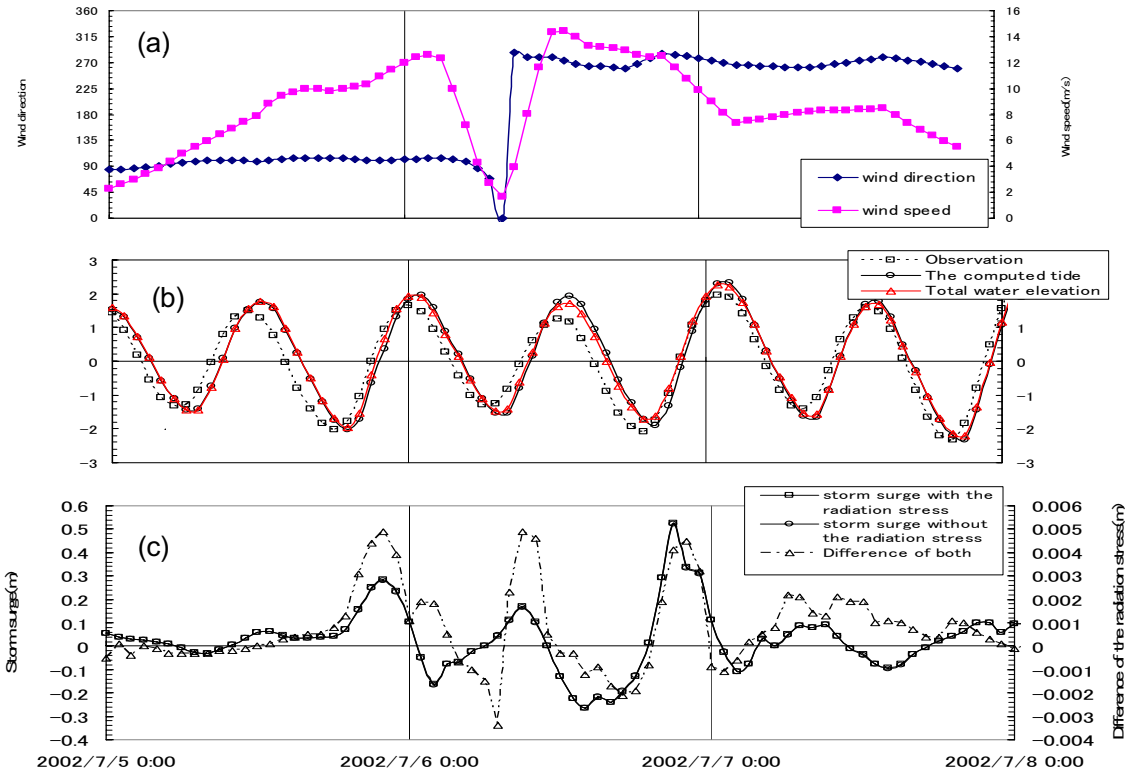

Figure 8. The same with Fig. 5 but at C (Boryeong)

References

Booij, N., R. C. Ris, and L. H. Holthuijsen (1999): A third-generation wave model for coastal regions. Part 1, Model description and validation, Journal of Geophysical Res., Vol.104, No.C4, pp. 7649-7666.

Choi, B. H., Hyun Min Eum, Seung Buhm Woo (2003): A synchronously coupled tide-wave-surge model of the Yellow Sea, Journal of Coastal Engineering, 47, pp. 381-398

Grant, W.D., Madsen, O.S (1986): The continental shelf bottom Boundary layer. Annu. Rev. Fluid Mech. 18, 265-305.

Janssen, P. A. E. M. (1989): Wave-induced stress and the Drag of Air Flow over Sea Waves, J. Phys. Oceanogr., 19, pp. 745-754.

Janssen, P. A. E. M. (1991): Quasi-linear Theory of Wind-Wave Generation Applied to Wave Forecasting, J. Phys. Oceanogr., 21, pp. 1631-1642.

Kagan, B.A., O. Alvarez, A. Izquierdo (2005): Weak wind-wave/tide interaction over fixed and moveable bottoms: a formulation and some preliminary results, Continental Shelf Research, 25, pp. 753-773.

Matumoto, K., T. Takanezawa and M. Ooe (2000): Ocean Tide Models Developed by Assimilating TOPEX/POSEIDON Altimeter Data into Hydro-dynamical Model: A Global Model and A regional Model around Japan, Journal of Oceanography, Vol.56, pp 567-581.

Mastenbroek, C., G. Burgers, and P. A. E. M. Janssen (1993): The Dynamical Coupling of a Wave Model and a Storm Surge Model through the Atmospheric Boundary Layer, J. Phys. Oceanogr., 23, pp. 1856-1866.

Ozer, Jose., Roberto Padilla-Hernandez., Jaak Monbaliu., Enrique Alvarez Fanjul., Juan Carlos Carretero Albiach., Pedro Osuna., Jason C. S. Yu., Judith Wolf (2000): A coupling module for tides, surges and waves, Journal of Coastal Eng., 41, pp. 95-124

Zhang, M. Y., and Y. S. Li (1995): The synchronous coupling of a third-generation wave model and a two-dimensional storm surge model, Journal of Ocean Eng., Vol.23 No.6, pp. 533-543

高潮に及ぼす大潮汐変動の影響

金　洙列*・高山知司・安田誠宏

*京都大学大学院工学研究科

要　旨

本研究は，海底地形が複雑で潮汐変動が大きい韓国の西側沿岸における高潮への大潮汐変動の影響を調べるものである。高潮は，様々な潮汐の時にランダムに発生するために，大潮汐変動は浅くて広い海域における高潮の大きさに強く影響すると考えられる。そこで，高潮／潮汐モデルと波浪モデル（SWAN）の結合モデルを構築し，相互にデータ交換ができるようにしている。このモデルを用いて，高潮と潮汐の関係とラディエーションストレスへの大潮汐変動の影響を調べた。 結合モデルを2002年に韓国西部を襲った台風Rammasunの追算に適用した。結合モデルによる計算の結果，高潮と潮汐の関係は線形的でなく，互いに強く影響し合うことがわかった。

キーワード：高潮，潮汐，ラディエーションストレス，結合モデル，SWAN